Eur. Phys. J. D **8**, 251–264 (2000)

THE EUROPEAN PHYSICAL JOURNAL D

EDP Sciences

Mesoscopic and macroscopic dipole clusters: Structure and phase transitions

A.I. Belousov[a] and Yu.E. Lozovik[b]

Laboratory of Nanophysics, Institute of Spectroscopy, Russian Academy of Sciences, Troitsk, 142092, Moscow region, Russia

Received 22 April 1999 and Received in final form 13 July 1999

Abstract. A two dimensional (2D) classical system of dipole particles confined by a quadratic potential is studied. This system can be used as a model for rare electrons in semiconductor structures near a metal electrode, indirect excitons in coupled quantum dots etc. For clusters of $N \leq 80$ particles ground state configurations and appropriate eigenfrequencies and eigenvectors for the normal modes are found. Monte-Carlo and molecular dynamic methods are used to study the order-disorder transition (the "melting" of clusters). In mesoscopic clusters ($N < 37$) there is a hierarchy of transitions: at lower temperatures an intershell orientational disordering of pairs of shells takes place; at higher temperatures the intershell diffusion sets in and the shell structure disappears. In "macroscopic" clusters ($N > 37$) an orientational "melting" of only the outer shell is possible. The most stable clusters (having both maximal lowest nonzero eigenfrequencies and maximal temperatures of total melting) are those of completed crystal shells which are concentric groups of nodes of 2D hexagonal lattice with a number of nodes placed in the center of them. The picture of disordering in clusters is compared with that in an infinite 2D dipole system. The study of the radial diffusion constant, the structure factor, the local minima distribution and other quantities shows that the melting temperature is a nonmonotonic function of the number of particles in the system. The dynamical equilibrium between "solid-like" and "orientationally disordered" forms of clusters is considered.

PACS. 61.46.+w Clusters, nanoparticles, and nanocrystalline materials – 68.65.+g Low-dimensional structures (superlattices, quantum well structures, multilayers): structure, and nonelectronic properties – 36.40.Ei Phase transitions in clusters

1 Introduction

The properties of a set of physical systems can, under certain conditions, be studied with the help of the model system of interacting dipoles. Particularly, it is a dipole-dipole interaction that is of main importance when small dielectric particles on the surface of an electrolyte [1] or monolayers of adsorbed atoms [2] are considered.

Another class of systems in which the majority of interesting properties is due to a dipole character of interaction are electron systems in semiconductors of small size located in the vicinity of a metal electrode. It is obvious that if the dot of a large enough size is situated near a single metal gate the electrostatic image forces will play an important role [3,4] and the long-ranged electron-electron Coulomb interaction potential will transform to the short-ranged dipole-dipole one between "composite" particles "electron + image charge". Recent advances in microlithography and one-electronics revived interest in such semiconductor structures, interesting because of the strong structural sensitivity to the number of particles [5,6]. One can suppose that such sensitivity makes possible a modulation of different thermodynamic properties and the temperatures of disordering in semiconductor structures through the addition of particles, and it also suggests the existence of unusual structural rearrangements with increasing temperature which, in turn, can lead to very interesting phenomena, for both theory and experiment, of coexistence between different types of ordered structures.

The main purpose of the present paper is to study, *via* detailed Monte-Carlo (MC) and molecular dynamic (MD) calculations, the ground state properties, temperatures and possible types of disordering phenomena of the system of electrons in a 2D semiconductor dot near a metal electrode, when the particles interact by a dipole law. We analyze the ground state structure of systems consisting of a finite number of dipoles ($N \leq 80$) in a harmonic confinement and the picture of their melting with increasing temperature. It turns out that on the basis of the character of disordering ("melting") phenomena dipole clusters can be divided into "mesoscopic" and "macroscopic" groups. In "mesoscopic" clusters of small numbers of particles ($N < 37$) there are two stages of disordering: orientational intershell disordering of different pairs of shells

[a] e-mail: bel_i_a@mail.ru
[b] e-mail: lozovik@isan.troitsk.ru

and, at greater temperatures, radial disordering when particles begin to interchange between shells. Increasing the temperature of large particle number clusters ($N > 37$) leads to radial disordering and to disruption of the shell structure at a temperature which is a function of the distance from the center of the system.

An analysis of the behaviour of different thermodynamic properties enables us to make a conclusion about the strong dependence of both "orientational" melting temperatures of mesoscopic and total disordering temperature of macroscopic clusters on the distribution of particles over crystal shells of different symmetry which can be associated with different parts of a perfect hexagonal crystal lattice. It is shown that clusters with the maximal number of completed crystal shells have anomalously high disordering temperatures.

As an intermediate between mesoscopic and macroscopic systems the cluster of 37 particles is considered. The most interesting feature of this cluster is the presence of the temperature region of coexistence of "solid-like" and orientationally disordered forms. This behavior of the system with increasing temperature is much like the picture of structural transitions in magic number atomic clusters [7–9].

The paper is organized as follows. In Section 2 we describe the model and briefly outline the methods that where used to find global minima configurations and to calculate different thermodynamic properties. Section 3 is devoted to the description and discussion of ground state configurations. In Section 4 we present the results from MC and MD simulations at different temperatures and system sizes. We consider two cases: "mesoscopic" ($N < 37$, see Sect. 4.1) and "macroscopic" ($N > 37$, see Sect. 4.2) clusters. Separately, as an intermediate case, in Section 4.3 we study the cluster of $N = 37$ particles. Our conclusions are presented in Section 5.

2 The model. Numerical simulation

We consider a semiconductor quantum dot situated within a single metal electrode (experimental realization of such systems is described, *e.g.*, in Ref. [5]). Due to the presence of electrostatic images of each electron, when the density of electrons n is small ($n \ll h^{-2}$, where h is the thickness of the spacer between the dot and the metal gate), the majority of system properties can be captured by a model system of interacting dipoles in a confining potential. Note that the concept of electrostatic image charges (*i.e.* electrostatic approximation for the polarization) is applicable at "large" h, when effects like the dynamical retardation of the polarization are negligible (see *e.g.* Ref. [10]). The dipole momenta of such "composite" dipole particles "electron + image charge" can be estimated as $d = eh$.

We consider the classical limit of the dipole cluster, when the amplitude of the quantum fluctuations is much smaller than the mean interparticle distance. The Hamiltonian for such a system, in the case of parabolic confinement with strength α, has the form

$$H = \sum_{i<j} \frac{d^2}{|\mathbf{r}_i - \mathbf{r}_j|^3} + \alpha \sum_{i=1}^{N} |\mathbf{r}_i|^2.$$

The Hamiltonian can be written in a dimensionless form if we express the coordinates and energy in the following units: $r_0 = d^{2/5}/\alpha^{1/5}$, $E_0 = \alpha r_0^2$. In such units the Hamiltonian becomes

$$H = \sum_{i<j} \frac{1}{|\mathbf{r}_i - \mathbf{r}_j|^3} + \sum_{i=1}^{N} |\mathbf{r}_i|^2. \quad (1)$$

From here on all the results will be given in the units introduced above. When considering thermodynamic properties of the system we will use the dimensionless temperature $T = k_{\mathrm{b}}T/E_0$.

In order to improve the reliability of results, all the ground state configurations presented below (see Tab. 1) were independently obtained with the help of two algorithms: "classical simulated annealing" [11] and "combined Monte-Carlo + gradient search" (see below). For each N we considered as many as 200 random initial configurations. This approach made it possible to study local minima as well as appropriate regions of catchment ("relative weights" of local minima).

In view of intrinsic statistical nature of the CSA method, the problem of localization of the system in local minima is solved in this approach much more easily than in different gradient methods. When using CSA, the system is modelled at some artificially introduced temperature $T(t)$ which is gradually decreased with the time t of experiment. This makes it possible to simulate the thermal noise and delocalize the system from metastable states. After starting from sufficiently high temperature of $T(t = 0) = 10$, at each t we performed ~ 200 MC steps per particle, whereupon the temperature was being decreased as $T(t + 1) = 0.98T(t)$. The trial move $\mathbf{x} \to \mathbf{x} + \delta\mathbf{x}$ at each MC step was generated in accordance with Gaussian probability distribution $\Pi(\delta\mathbf{x}) \sim \exp(-\delta\mathbf{x}^2/T(t))$. This move was accepted with the probability $p = \min\{1, \exp(-\Delta E/T(t))\}$. Several hundreds of conjugate gradient steps were performed at the last stage of the algorithm to gain in the accuracy of results.

It turned out that CSA is not as fast an algorithm as the *combined MC + gradient search* method. A search for minima within the last approach consists of repeated (up to 10^4 combined moves) applying the following procedures:

(1) classical random search when the trial move $\mathbf{r} \to \mathbf{r}+\delta\mathbf{r}$ is accepted if it reduces the energy. The maximal size of the trial move $\max\{|\delta\mathbf{x}|\}$ was chosen automatically to assure the acceptance probability of a new configuration of 0.1;
(2) gradient search method $\mathbf{r} \to \mathbf{r} - \gamma\nabla H$, $\gamma \approx 0.01$;
(3) "Ravine" method [12]. In this method the direction $\mathbf{l}$ of the most probable displacement of the system that moves in a long narrow ravine is predicted on the basis

Table 1. Ground state configurations of 2D dipole clusters D_N in a harmonic confining. Shown are shell configurations $\{N_1, N_2, ...\}$, types of crystal shells (see in text) and excess energy $\epsilon = E/N$.

N	$\{N_1, N_2, ...\}$		ϵ	N	$\{N_1, N_2, ...\}$		ϵ
1	1		0	41	$\underline{3,9},14,15$	Cr_3	8.93397
2	2		0.64660	42	$\underline{3,9},14,16$	Cr_3	9.08148
3	3		1.01394	43	$\underline{3,9,15},16$	Cr_3	9.22705
4	4		1.38021	44	$\underline{3,9,15},17$	Cr_3	9.37309
5	5		1.75713	45	$\underline{4,10},15,16$	Cr_4	9.51691
6	$1,5$		2.04829	46	$\underline{4,10},15,17$	Cr_4	9.66006
7	$\underline{1,6}$	Cr_1	2.32591	47	$\underline{4,10,16},17$	Cr_4	9.80303
8	$1,7$	Cr_1	2.63542	48	$\underline{4,10,16},18$	Cr_4	9.94353
9	$2,7$	Cr_2	2.92373	49	$1,5,11,16,16$	Cr_1	10.08318
10	$3,7$	Cr_3	3.19012	50	$\underline{1,6},11,16,16$	Cr_1	10.21803
11	$3,8$	Cr_3	3.41972	51	$\underline{1,6,12},16,16$	Cr_1	10.35593
12	$\underline{3,9}$	Cr_3	3.66665	52	$\underline{1,6},11,17,17$	Cr_1	10.49035
13	$4,9$	Cr_4	3.89493	53	$\underline{1,6,12},17,17$	Cr_1	10.62096
14	$\underline{4,10}$	Cr_4	4.13543	54	$\underline{1,6,12},17,18$	Cr_1	10.75525
15	$5,10$		4.35999	55	$\underline{1,6,12,18},18$	Cr_1	10.88617
16	$1,5,10$		4.56558	56	$\underline{1,6,12,18},19$	Cr_1	11.02094
17	$\underline{1,6},10$	Cr_1	4.77272	57	$\underline{1,6,12,18},20$	Cr_1	11.15521
18	$\underline{1,6},11$	Cr_1	4.97257	58	$\underline{1,6,12,18},21$	Cr_1	11.28939
19	$\underline{1,6,12}$	Cr_1	5.18009	59	$\underline{2,8},13,18,18$	Cr_2	11.41878
20	$1,7,12$	Cr_1	5.38833	60	$3,8,13,18,18$	Cr_3	11.54741
21	$2,7,12$	Cr_2	5.59048	61	$\underline{2,8,14},18,19$	Cr_2	11.67875
22	$\underline{2,8},12$	Cr_2	5.77969	62	$\underline{2,8,14},19,19$	Cr_2	11.80329
23	$3,8,12$	Cr_3	5.96866	63	$3,8,14,19,19$	Cr_3	11.92863
24	$3,8,13$	Cr_3	6.14713	64	$\underline{3,9},14,19,19$	Cr_3	12.05160
25	$\underline{3,9},13$	Cr_3	6.32561	65	$\underline{3,9,15},19,19$	Cr_3	12.17598
26	$4,9,13$	Cr_4	6.50834	66	$\underline{3,9},14,20,20$	Cr_3	12.30108
27	$4,9,14$	Cr_4	6.68410	67	$\underline{3,9,15},20,20$	Cr_3	12.42251
28	$\underline{4,10},14$	Cr_4	6.85654	68	$\underline{3,9,15},20,21$	Cr_3	12.54674
29	$5,10,14$		7.03598	69	$\underline{4,10},15,20,20$	Cr_4	12.66865
30	$5,10,15$		7.20543	70	$5,10,15,20,20$		12.78866
31	$1,5,10,15$	Cr_1	7.36745	71	$1,5,10,15,20,21$		12.90960
32	$\underline{1,6,12},13$	Cr_1	7.52917	72	$\underline{4,10,16},21,21$	Cr_4	13.03147
33	$\underline{1,6,12},14$	Cr_1	7.68741	73	$1,5,11,16,20,20$		13.15305
34	$\underline{1,6,12},15$	Cr_1	7.84408	74	$1,5,11,16,21,20$		13.27021
35	$\underline{1,6,12},16$	Cr_1	8.00361	75	$1,5,11,16,21,21$		13.38454
36	$\underline{1,6,12},17$	Cr_1	8.16885	76	$\underline{1,6},11,16,21,21$	Cr_1	13.50135
37	$\underline{1,6},\tilde{1},13,16$	Cr_1	8.33111	77	$\underline{1,6,12,18},20,20$	Cr_1	13.61939
38	$\underline{2,8},13,15$	Cr_2	8.48550	78	$\underline{1,6,12},17,21,21$	Cr_1	13.73279
39	$3,8,13,15$	Cr_3	8.63869	79	$\underline{1,6,12,18},21,21$	Cr_1	13.84553
40	$\underline{3,9},14,14$	Cr_3	8.78617	80	$\underline{1,6,12},17,22,22$	Cr_1	13.96137

of a series $\{\mathbf{r}_1, \mathbf{r}_2, ... \mathbf{r}_m\}$ of successive gradient search steps: $\mathbf{l} = \mathbf{r}_m - \mathbf{r}_1$. A number of trial moves in this direction $\mathbf{r} \to 0.5(\mathbf{r}_1 + \mathbf{r}_2) + \mathbf{l}\delta$ completes the method. The maximal size of these moves $\max\{|\delta|\}$ was adjusted in such a way as to achieve the acceptance probability of ~ 0.1. We found that the throughput of the combined method was maximal when moves of above-mentioned types where performed in the ratio of $N_1 : N_2 : N_3 = 100 : 10 : 2$.

When studying the thermodynamic properties of the system, we used the Metropolis Monte-Carlo algorithm [13]. For the system of small number of particles ($N < 40$) and at sufficiently low temperatures ($T < 0.02$), when shells are well defined, we found it very efficient to perform collective MC moves of different shells. With the multigrid approach [14] for shell s of N_s particles one can apply the following types of collective moves with wave vector k_s:

(1) angular perturbations such that angles φ_{i_s} of particles which belong to shell s vary as

$$\varphi_{i_s} \to \varphi_{i_s} + \xi\delta_\varphi(k; s)\cos(2\pi k i_s/N_s) \qquad (2)$$

with ξ being the random variable uniform in $[-1, 1)$;

(2) radial perturbations of shell s:

$$r_{i_s} \to r_{i_s} + \xi\delta_r(k; s)\cos(2\pi k i_s/N_s). \qquad (3)$$

Parameters δ_φ and δ_r are adjusted in such a way as to assure a given acceptance probability of a new configuration.

It is obvious that the case $k_s = 0$ corresponds to the symmetrical "breathing" of shell s when the radial perturbation (3) is considered and to the rotation of the shell as a whole when one performs the global move (2). We found that such rotation of different shells was very important when studying the phenomena of intershell orientational disordering which take place in mesoscopic systems at low temperatures (the temperatures of orientational "melting" can be many orders less than that of full disordering and shells' destruction). The approach described above enabled us to increase the efficiency of calculations by about five times.

To study dynamical characteristics of the system we applied molecular dynamic simulations (both isokinetical and microcanonical methods where used). The main portion of the results presented below were obtained with the help of the fourth-order Runge-Kutta scheme. Equations of motion were integrated in $\sim 10^4$ MD steps of size $\tau \leq 0.01\tau_0$, where $\tau_0 = \sqrt{m^*/\alpha}$ determines the time scale in the system.

3 Ground state configurations

Previous studies of Coulomb [15–18] and logarithmic [19–21] clusters have shown that it is suitable to classify ground state configurations of these finite systems in accordance with their shell structure. Differences between structures of two-dimensional dipole (D) and Coulomb clusters can be seen even at $N = 10$ (the system D_{10} has the structure $D_{10}(3, 7)$ as distinct from $(2, 8)$ for Coulomb system [22]). The number of differences grows rapidly with increasing number of particles. To explore tendencies in the process of cluster shells developing, let us consider the shell configurations of 2D dipole clusters that are presented in Table 1 (see also Fig. 1). The results of calculations show that particles fill in shells which are not concentric to the perimeter of the cluster, the basis for most configurations is provided by different parts of 2D hexagonal lattice. This observation is not specific to clusters with short-ranged pair interactions only. As was argued by Koulakov and Shklovskii [6], only a narrow ring adjacent to the perimeter of sufficiently large 2D Coulomb clusters is concentric to it, the rest of the cluster is filled with an almost perfect crystal.

When describing and analyzing the properties of such configurations we found it suitable to introduce into consideration the "crystal shells" Cr_c that are concentric groups of nodes of ideal 2D crystal with c nodes placed in the center of these groups (see Fig. 2). Obviously, in view of the axial symmetry of the confinement potential, we can concentrate on a finite number of the most symmetrical crystal shells. By the number of particles in the center of the system, the crystal shells can be divided into the following groups: Cr_1, Cr_2, Cr_3, Cr_4. Figure 2 explains our definition. The number of particles N_s that belong to crystal shell s (crystal row) of type Cr_c is $N_s = c + 6(s-1) - \delta_{c1}(1 - \delta_{s1})$ (δ_{ij} is the Kronecker's symbol).

With the help of the crystal shell concept an analysis of the results presented in Table 1 shows that as the number of particles in the cluster increases, the configuration of the system changes in accordance with the following tendencies:

1. the maximum number of *crystal shells* is filled;
2. the number of particles on the last two shells tends to be equal.

To illustrate these tendencies we underline the shells which are filled up (see Fig. 1 and Tab. 1 where the types of basic crystal shells are also shown).

An addition of particles to the cluster leads to the completing of crystal shells of some type, followed by the structure rearrangement (Figs. 1c–1d) after which crystal shells of different type begin to fill. From Table 1 one can see that in some cases it is more advantageous to depart from the order $Cr_1 \to Cr_2 \to Cr_3 \to Cr_4$ in which different types of crystal shells appear. Examples of such deviations (*e.g.* $D_{56}-D_{61}$ and $D_{71}-D_{73}$) show that it can be profitable to reduce the number of particles on first shells (in the center of the system) and equalize them on the last ones. This observation underlines the importance of the requirement that the last two shells of the cluster have equal numbers of particles.

It is to be noted that for some systems the choice of the basis crystal group is ambiguous. The most spectacular examples of this ambiguity are clusters that we assign

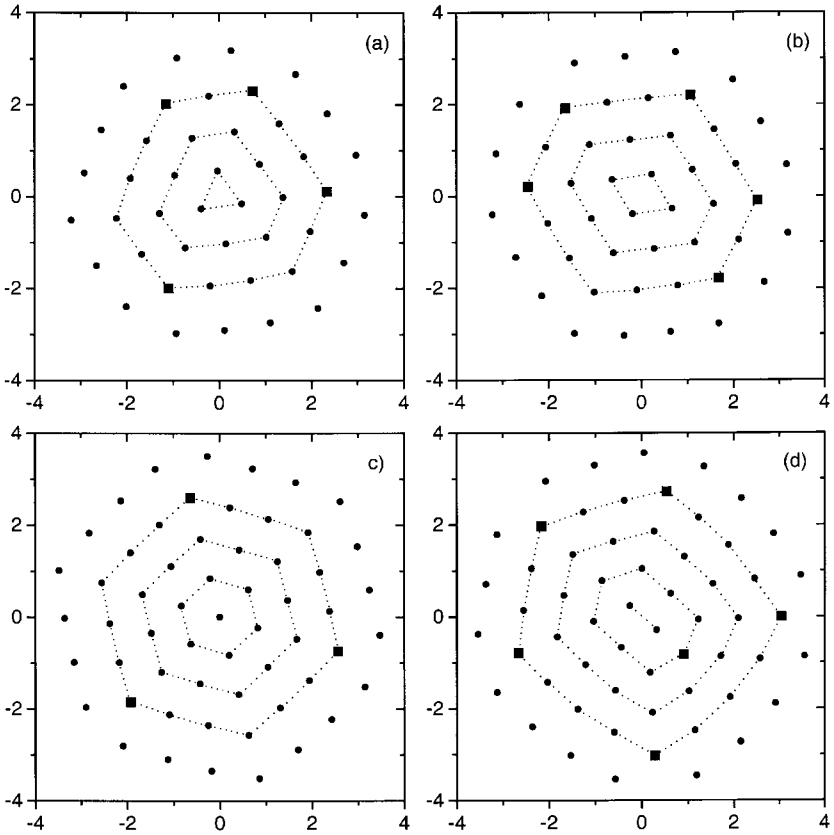

Fig. 1. Ground state configurations of some dipole clusters: (a) D_{44}; (b) D_{47}; (c) D_{58}; (d) D_{59}. Squares denotes particles with 5 nearest neighbors.

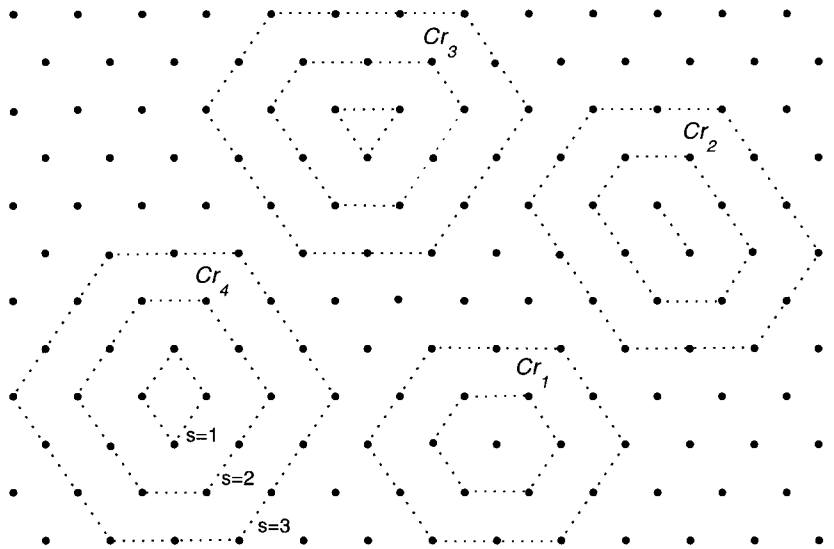

Fig. 2. Different parts of a 2D hexagonal lattice produce the basis for ground state configurations of the majority of dipole clusters (see Tab. 1). Shown are examples of such basic groups of crystal shells. The four most symmetrical groups of three shells each is presented.

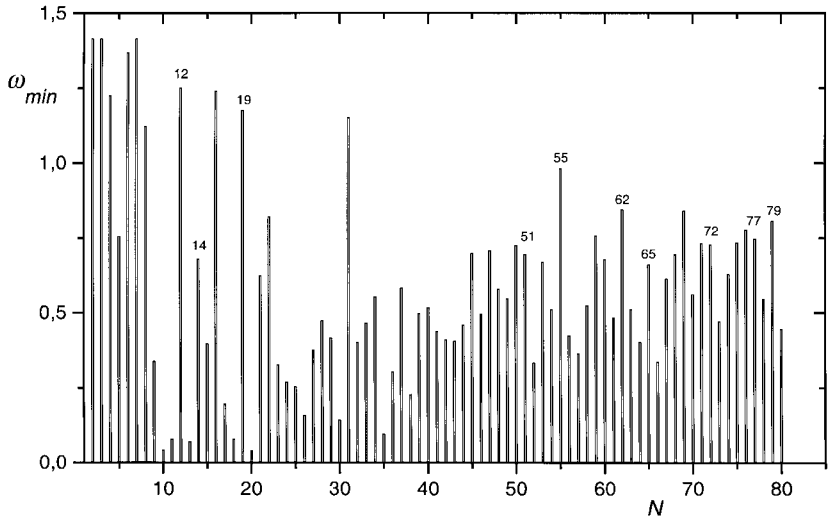

Fig. 3. Minimal nonzero eigenfrequencies $\omega_{\min}$ for the normal modes of N-particle dipole clusters.

to Cr_2 crystal group (such clusters are $D_{38}, D_{59}, D_{61}, D_{62}$, see Tab. 1). Of course, one can consider these systems as having a number of partially completed crystal shells of Cr_4 type (the "body" of a cluster) while the other particles locate on the surface of this "body". In breaking a cluster into shells we have been guided by the requirement that the outer shell of the cluster be well-defined and *closed*. For the system with a more short-ranged interaction potential (*e.g.* with the exponential or screened Coulomb interaction potential) it can be more natural to consider the evolution of the cluster with N as consisting of switching between *three* types of the most symmetrical basic crystal shells, namely Cr_1, Cr_3, Cr_4 [6]. Seemingly, the question of what approach is more adequate can be answered by the data of the thermodynamic and dynamic analysis.

Of a peculiar interest are the "magic" dipole clusters with the maximal number of completely filled crystal shells and, in the case of clusters of a large number of particles ($N > 40$), with equal number of particles on the last two shells. An analysis of Table 1 suggests that these clusters are $D_{12}, D_{14}, D_{19}, D_{36}, D_{40}, D_{51}, D_{54}, D_{55}, D_{62}, D_{65}$... The spectral analysis of the ground state configurations [16] shows that there is a correlation between the value of the minimal nonzero eigenfrequency $\omega_{\min}$ and the extent to which crystal shells are completed (see Fig. 3), the clusters with the maximal number of completed crystal shells (and equal number of particles on the last two shells) have, as a rule, maximal values of $\omega_{\min}$. To illustrate this statement we have calculated the correlation coefficient between the minimal nonzero eigenfrequency $\omega_{\min}(N)$ and the degree to which a given cluster can be thought of as a "magic" one, *m(N) = ("the number of filled crystal shells" + 1 if the number of particles in the last two shells are equal) / ("the number of cluster shells").* We found that $\mathrm{corr}(\omega_{\min}, m) \approx 0.22 > 0$ in the region $N \in [10, 80]$, which is indicative of the correlation supposed.

At the end of this section let us discuss the arrangement of particles into shells in the cluster D_{37} (see Fig. 4). One can see that one of the particles is between the second and the third shell to form an interstitial (it is analogous to the Frenkel defect in crystals). Such classification of this particle is based on the Voronoi analysis which shows that the central particle has six neighbours. The corresponding configuration can be denoted by $D_{37}(\underline{1,6},\tilde{1},13,16)$ where the tilde stands for the interstitial.

It is pertinent to note that the presence of interstitials is common with 3D Coulomb clusters as the number of particles becomes of the order of several hundreds [18]. As have been observed, it is typically the case that, due to the presence of such interstitial charges caught between concentric shells, the inner shells of large 3D systems are less well defined than the outer ones.

There exist also other opportunities to describe the structure of the cluster D_{37}, for example as $D_{37}(\underline{1,6,12},\tilde{2},16)$. Our choice (see also Tab. 1 and Fig. 4a) has also proved itself in the results of the analysis of the lowest local minima configuration that has well-defined shell structure: $D_{37}^{(1)}(1,7,13,16)$ This configuration is shown in Figure 4a. It will be shown below that the ground state configuration peculiarities of the cluster involved lead to rather a complex picture of disordering phenomena with increasing temperature.

4 Phase transitions

4.1 Mesoscopic clusters (N < 37)

The distinctive property of mesoscopic clusters is the presence of *two types* of disordering effects in these systems: [15,21,22] an intershell orientational disordering (an orientational melting of shells s_1 and s_2 at temperature $T_{s_1 s_2}$) and a radial disordering (a total melting at temperature T_{m} that is larger than any one of the orientational melting temperatures). An analysis of eigenfrequencies and eigenvectors for the normal modes of small clusters shows that the motions with small lowest nonzero eigenfrequencies $\omega_{\min}$ correspond to intershell rotation. Such clusters will

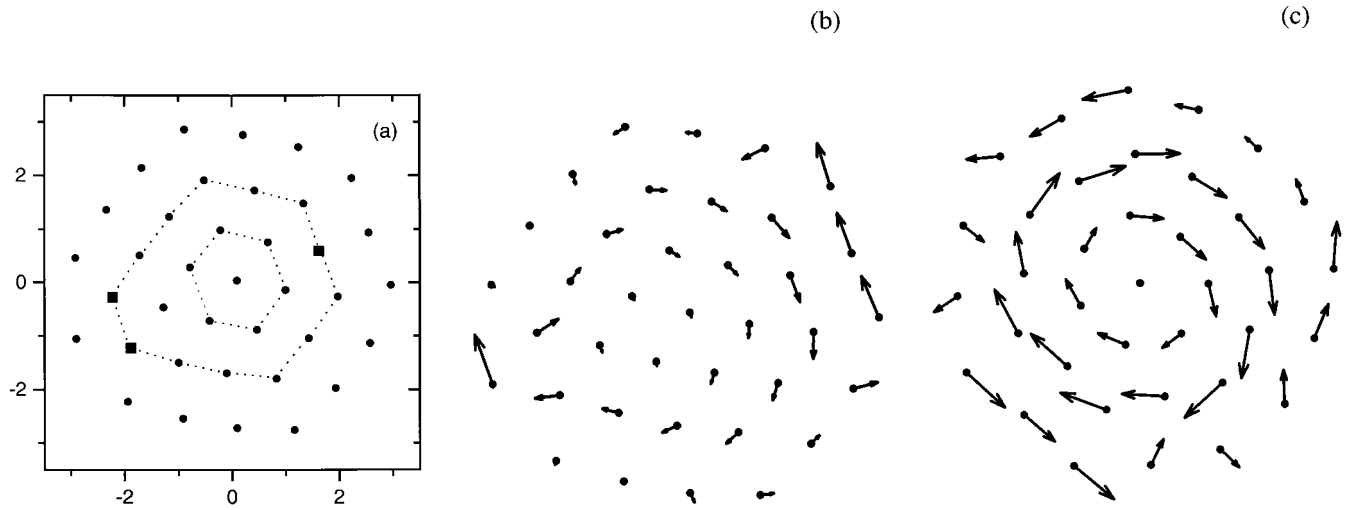

Fig. 4. Cluster D_{37}. (a) The ground state configuration $D_{37}(\underline{1,6},\tilde{1},13,16)$. (b) The eigenvector of the cluster motion in the global minimum with the minimal nonzero eigenfrequency $\omega_{\min} \approx 0.58$. (c) The picture of the motion in the lowest local minimum $D_{37}^{(1)}(1,7,13,16)$ with a minimal eigenfrequency $\omega_{\min}^{(1)} \approx 0.4$. Five-coordinated particles are marked by squares.

have small temperatures $T_{s_1 s_2}$ of intershell disordering, at which shells start to rotate relative to each other losing their mutual orientational order. Note that, in contrast to the case of large clusters, an intershell melting in small clusters takes place for *all* pairs of shells, *i.e.* there exist "melting" temperatures T_{21}, T_{32}, T_{43}... In clusters of large numbers of particles ($N > 37$) an orientational disordering of only the outer shell is possible. An analogous observation was made for Coulomb clusters [16].

The usual way of studying the intershell orientational disordering in 2D repulsive clusters is an analysis of relative angle deviations of shells (in analogy with pair deviations (6), see below) [15,16,21,22]. In this approach the temperature $T_{s_1 s_2}$ of orientational "melting" of cluster shells s_1 and s_2 is defined as that at which there is a sharp increase in the value of appropriate relative angle deviations. We define the temperature $T_{s_1 s_2}$ of orientational "melting" of shells s_1 and s_2 as that at which the *mutual orientational (order) parameter* of shells s_1 and s_2 vanishes [23]. We introduce this quantity as follows: for each shell s of N_s particles we consider the complex-valued quantity ψ_s:

$$\psi_s = \frac{1}{N_s} \sum_{i_s} \exp\left(\jmath N_s \varphi_{i_s}\right). \tag{4}$$

The sum in (4) is extended over all particles from shell s. The *mutual orientational (order) parameter* is then defined as

$$g_{s_1 s_2} = \langle \psi_{s_1} \psi_{s_2}^* \rangle. \tag{5}$$

It is obvious, that $g_{s_1 s_2}$ disappears at the point of relative disordering (slipping) of shells s_1 and s_2, $g_{ss} = \langle |\psi_s|^2 \rangle$ can be considered as a measure of the intrashell order.

The orientational order parameter ψ_s discussed above is a special case of the more general orientational bond-order parameter $Q_6(\mathbf{r})$ widely used for 3D clusters and bulk systems [9,24]. In this connection it is worth while to note, that both $Q_6(\mathbf{r})$ and ψ_s are natural generalizations of two-dimensional hexatic parameter $\psi_6(\mathbf{r})$ [25]. The mutual orientational (order) parameter $g_{s_1 s_2}$ is analogous to the correlation function $g_6(r)$ of an infinite 2D system, where vanishing (when the translational order is absent) of the correlation function, $g_6(r) \to 0$ as $r \to \infty$, indicates the relative orientational disordering of distant parts of a system.

Shown in Figure 5 are dependencies of the values of mutual orientational parameters g_{21} and g_{32} *vs.* temperature for three-shell cluster D_{24}. Also plotted are pair and radial deviations $\delta_{\text{pair}}(T)$ and $u_{\text{r}}^2(T)$

$$\delta_{\text{pair}} = \frac{2}{N(N-1)} \sum_{i<j} \left[\frac{\left\langle |\mathbf{r}_i - \mathbf{r}_j|^2 \right\rangle}{\left\langle |\mathbf{r}_i - \mathbf{r}_j| \right\rangle^2} - 1 \right]^{1/2} \tag{6}$$

$$\delta_{\text{r}} = \frac{1}{N} \sum_{i}^{N} \left[\frac{\left\langle |\mathbf{r}_i|^2 \right\rangle}{\left\langle |\mathbf{r}_i| \right\rangle^2} - 1 \right]^{1/2},$$

$$u_{\text{r}}^2 = \frac{1}{N} \sum_{i}^{N} \left[\left\langle |\mathbf{r}_i|^2 \right\rangle - \left\langle |\mathbf{r}_i| \right\rangle^2 \right]. \tag{7}$$

The figure shows that for cluster D_{24} one can define two temperatures $T_{32} = (5 \pm 0.5) \times 10^{-4}$ and $T_{21} = (3 \pm 0.05) \times 10^{-4}$ which correspond to orientational melting of shells $\{3,2\}$ and $\{2,1\}$.

Figure 5 (see also Fig. 6) shows that pair and radial deviations (6, 7) are also sensitive to intershell rotation. One can see the regions of sharp increases in the values of these quantities that coincide with the regions of vanishing of mutual orientational order. The sensitivity of radial and pair deviations to the orientational disordering is due to the "breathing" of the cluster shells on their rotation. This breathing can be clearly seen if one traces the motion of a system along a "reaction path" [26], the most probable trajectory which is appropriate to the intershell rotation.

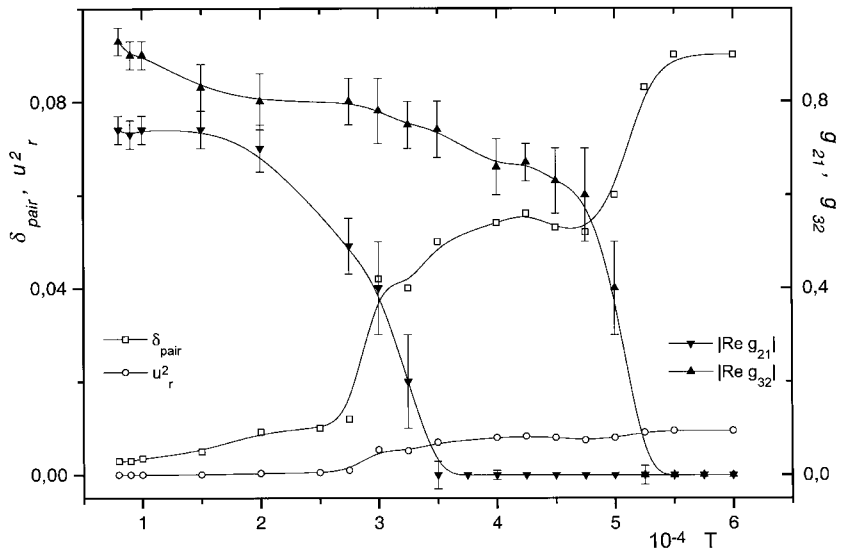

Fig. 5. Three-shell cluster $D_{24}(3, 8, 13)$. The results of calculations of the mutual orientational parameter (5) and of deviations (6, 7) as functions of temperature T are presented. The data are connected to guide the eyes. If not present, error bars are smaller than the size of the data point.

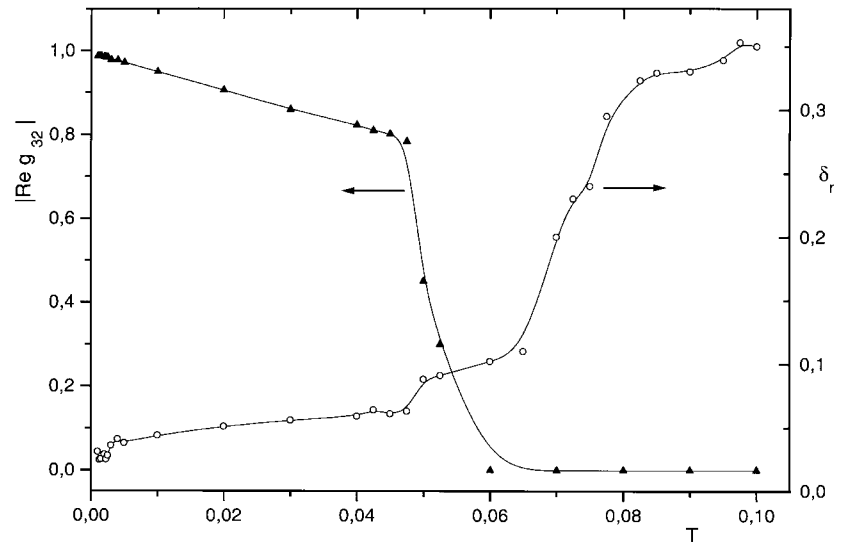

Fig. 6. Four-shell cluster $D_{35}(\underline{1, 6, 12}, 16)$. Mutual orientational parameter $\mathrm{Re}|g_{32}|$ and relative deviations $\delta_{\mathrm{pair}}(T)$ *vs.* temperature T.

Temperature $T_{32} \approx 0.05 \pm 0.003$ of the orientational "melting" of the third shell of four-shell cluster $D_{35}(\underline{1, 6, 12}, 16)$ is only slightly lower than the temperature $T_{\mathrm{m}} = 0.065 \pm 0.005$ of the total melting at which the radial order disappears (see Fig. 6). It is obvious that the temperature of an orientational intershell disordering will to a large extent depend on the distribution of particles throughout shells. Particularly, as a pair $\{s_1, s_2\}$ of completed crystal shells is considered (see Sect. 3), appropriate temperature $T_{s_1 s_2}$ of an orientational "melting" should be maximal (irrespective of whether these shells are inside the cluster or a pair of external shells is considered). Calculations do show that the addition of as little as one particle to small cluster $D_{19}(\underline{1, 6, 12})$ with completely filled crystal shells of Cr_1 type leads to abrupt decreasing of temperature T_{32} of orientational "melting". Indeed, temperature $T_{32} \approx 0.03 \pm 0.002$ of D_{19} cluster is very nearly equal to that of the total melting $T_{\mathrm{m}} \approx 0.038 \pm 0.003$ (at which particles begin to interchange between shells). System $D_{20}(1, 7, 12)$ becomes orientationally disordered at much smaller temperatures $T_{32} < 5 \times 10^{-6}$.

To conclude this section, we would like to sketch the differences between the results presented here and that of previous examinations of 3D Coulomb clusters in a symmetrical harmonic trap. The study of potential energy surfaces, spectra and barriers for rearrangements of different types has shown [17,18] that the rearrangements of 3D clusters can be classified as intershell or intrashell,

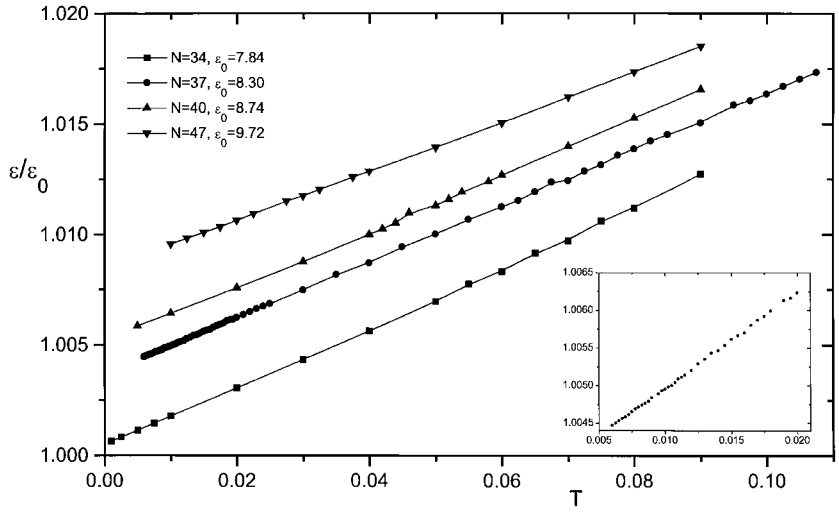

Fig. 7. Temperature dependence of excess energy $\epsilon(T)$ for a number of dipole clusters D_N. Shown on an enlarged scale is the excess energy of D_{37} cluster in the temperature region $T \in [0.005, 0.02]$ (to be compared with the results of work [22]).

where intrashell processes involve permutations of atoms belonging to the same shell of the cluster (*i.e.* the surface diffusion over concentric shells may take place). In contrast, 2D repulsive clusters do not reveal any intrashell disordering phenomena. Instead, all the rearrangements are intershell ones and involve both migration of particles between different shells of a cluster and mutual orientational disordering (slipping) of different pairs of internally ordered shells.

4.2 Macroscopic clusters (N > 37)

The most interesting when considering macroscopic clusters (at $N > 37$) is the question about the manner in which their melting temperatures $T_{\rm m}$ approach the temperature [27,28] $T_{\rm m}^{\rm inf} = k_{\rm b}T_{\rm m}/(d^2n^{3/2}) = 0.089 \pm 0.002$ of first order phase transition in 2D infinite dipole system (here n stands for the density of particles in the system [29]).

One of the most representative quantities for 2D infinite dipole system is excess energy ϵ that exhibits a jump of $\Delta\epsilon \approx 0.04$ at a temperature of phase transition $T_{\rm m}^{\rm inf}$ [27]. Our calculations show (see Fig. 7) that such a sharp increase in an excess energy does not take place at least for clusters with $N < 50$. We think this peculiarity is primarily connected with the incommensurability of the circular shape of the trap with the lattice and the inhomogeneity of the particle density. Later we will discuss this question in some more detail.

Yet another quantity that is commonly used in analyzing phase transitions in infinite systems is the structure factor $S(\mathbf{k}) = 1/N\langle\rho_{\mathbf{k}}\rho_{-\mathbf{k}}\rangle$, $\rho_{\mathbf{k}} = \sum_i \exp(j\mathbf{k}\mathbf{r}_i)$. The lattice to liquid transition is identified through the vanishing of the first Bragg peak $S(\mathbf{k})$, $\mathbf{k} \approx \mathbf{q}_1$. We found that the magnitude of this peak (the maximum of the structure factor in the region $|\mathbf{k}| > k_{\rm c} \sim \pi$) is acutely sensitive to the disordering in clusters. The peak at small wave vectors $|\mathbf{k}| < \pi$ that exists at any temperature due to finite size of the system involved is of no interest. Some characteristic examples of the behavior of the structure factor as a function of temperature are given in Figure 8.

An independent quantity, a sharp change in which testifies about the order/disorder transition, is the radial diffusion constant $\mathcal{D}_{\rm r}$. Figure 9 presents the results of calculations of this quantity, performed for clusters D_{39}, D_{40} and D_{45}. Each data point in this figure was obtained by averaging over results of 5 independent experiments in which the evolution of the system was observed in a time that is typical for the diffusion of a particle for a distance of $\Delta r \sim 1$. The result one of such experiment is shown in the inset of the figure.

From the analysis of temperature dependencies of the structure factor, relative deviations, and diffusion constant one can plot the total melting temperature $T_{\rm m}(N)$, $N \leq 52$ as a function of the number of particles in the cluster. This curve is shown in the inset of Figure 9. The figure enables us to point out some characteristic features of the N dependence of the disordering temperature. (i) Melting of all clusters studied takes place at temperatures much smaller than temperature $T_{\rm m}^{\rm inf} \approx 0.1$ of the phase transition in an infinite system. (ii) The function $T_{\rm m}(N)$ is nonmonotonic. An analysis of the data presented in Table 1 shows that the clusters with a maximal number of completed crystal shells have anomalously high melting temperatures (at least for $N < 52$). Most likely, this peculiarity is primarily connected with the fact that a cluster of N particles can be considered as a part of a *strongly distorted* crystal lattice. Hence one studies the melting of a part of the imperfect crystal with "frozen-in" interstitials and dislocations (see Fig. 1a), the melting temperature being a function of the number of such defects (of the value of an initial deformation of a cluster as a part of the crystal). Obviously, the number of defects in the ground state configuration will be minimal in the case of a cluster with a maximal number of filled crystal shells.

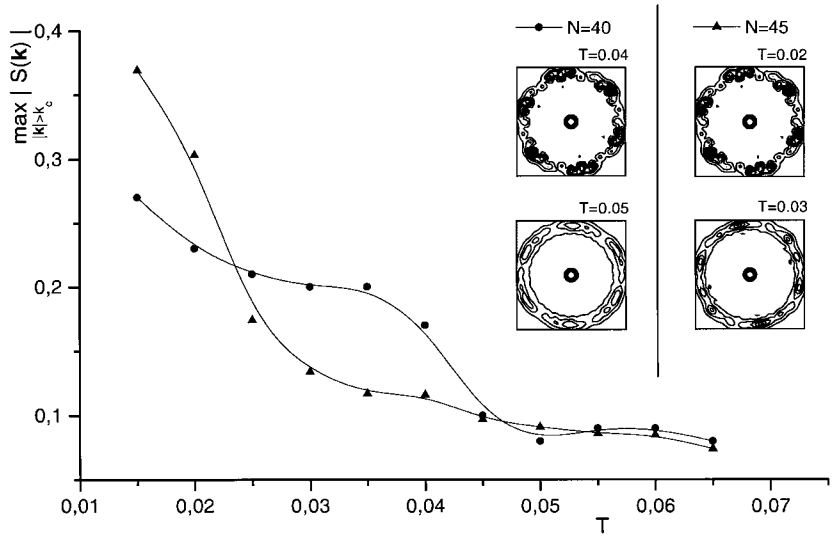

Fig. 8. The magnitude of the first Bragg peak as a function of T for clusters D_{40} and D_{45}. Shown also is 2D topography of the structure factor $S(\mathbf{k})$, $S(\mathbf{k}) < 0.5$ at different temperatures. "Solid-like" to "liquid-like" transition is accomplished by the washing out of $S(\mathbf{k})$ in regions $\mathbf{k} \approx \mathbf{q}_1$ of reciprocal lattice vectors.

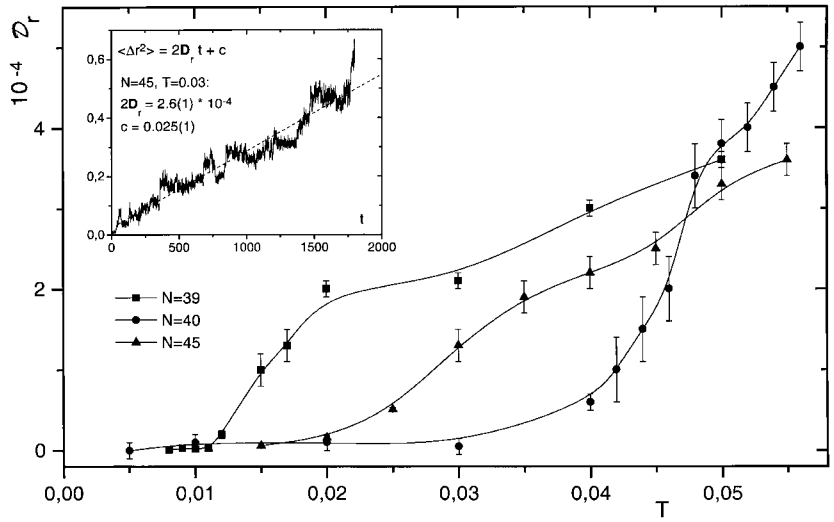

Fig. 9. The radial diffusion constant *vs.* temperature T. The inset shows a typical diffusive motion of particles when the cluster is in a disordered state ($T \geq T_{\mathrm{m}}$). Results of the linear fit are also given.

Of course, the melting temperature is not a strictly defined quantity for finite systems. It makes sense to consider an interval $\Delta T(N)$ of temperatures in which the disordering takes place. For clusters of large numbers of particles that repel each other and are in a confinement potential there is another, more important, reason that does not enable us to introduce the concrete temperature of a phase transition (of the total disordering in a system). The point is that large dipole clusters (at $N > 50$) are strongly irregular in both the density of particles and the density of defects. These densities can vary appreciably with the distance r to the center of the system to lead to r-dependence of the melting temperature.

Let us consider this question in some more detail. Results of numerical simulations show that large repulsive clusters in a confinement can be viewed as consisting of the following regions [6]: (a) the crystal "core", the region (belonging to a circle of some radius $r_{\mathrm{c}}(N)$) adjacent to the center of the cluster and filled with a number of completed crystal shells; (b) the outer region ($r > r_{\mathrm{c}}(N)$) in which dislocations and disclinations are situated. In order to account for the r-dependence of the local density of particles $n = n(r)$ when considering the temperatures of disordering of different parts of the cluster let us introduce the scaled to 2D infinite system temperature $T^{\mathrm{inf}}(r)$ as

$$T^{\mathrm{inf}}(r) = Tn(r)^{-3/2}. \tag{8}$$

Our calculations have shown that the scaled temperature of disordering of the "core" (of the region (a), see above) is *independent* of r and is slightly below the

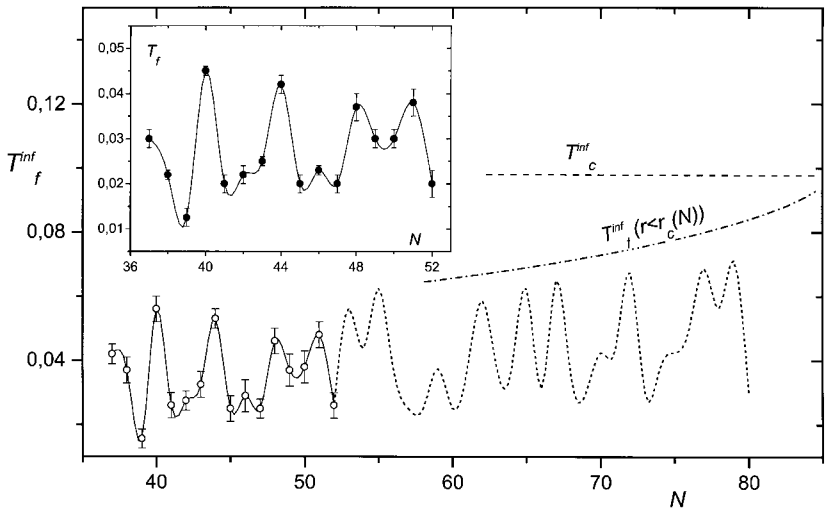

Fig. 10. The total melting temperatures $T_{\rm m}(N)$ and scaled [29] from "cluster" to "infinite system" temperatures $T_{\rm f}^{\rm inf}(N)$ as functions of number of particles N. Points correspond to the results of present simulations. The dotted line depicts a possible behavior of $T_{\rm f}^{\rm inf}(N)$ at $N > 50$. Temperature of first-order phase transition in an infinite 2D dipole system $T_{\rm m}^{\rm inf}$ is shown with the help of a dashed line. Temperature $T_{\rm m}^{\rm inf}(r < r_{\rm c}(N))$ (8) of the disordering of a core is assumed to tend to $T_{\rm m}^{\rm inf}$ as N increases.

temperature of the phase transition in an infinite 2D system. For example, considering the region $r < 2.5$ of D_{80} cluster we have found $T_{\rm m}^{\rm inf}(r < 2.5) = 0.07 \pm 0.01$. One can suppose that as N increases, the scaled temperature of core disordering $T_{\rm m}^{\rm inf}(r < r_{\rm c}(N))$ approaches the temperature of phase transition in a 2D infinite dipole system: $T_{\rm m}^{\rm inf}(r < r_{\rm c}(N)) \to T_{\rm m}^{\rm inf}$.

It is worth while to note that, being measured in the central region of the cluster D_{80}, the excess energy does have a small jump of $\delta\epsilon(r < 2.5) \approx 0.01$. Similar analysis was performed for a 2D logarithmic cluster of 500 particles in a harmonic confinement (all measurements were performed in the central part of the cluster) [30]. A reduction in the value of the excess energy jump with respect to that in a 2D infinite system was ascribed to the "boundary effects", the influence of the rest of the cluster.

Obviously, the temperature of disordering in the outer region (in the region (b)) strongly depends on the number of disclinations and dislocations in them and will be smaller of the disordering temperature of a core: $T_{\rm m}^{\rm inf}(r > r_{\rm c}) < T_{\rm m}^{\rm inf}(r < r_{\rm c})$. As for D_{80} cluster, the melting of their outer part was found to take place at $T^{\rm inf}(r > r_{\rm c}) = 0.01 \pm 0.005$.

Thus we argue that:

(i) defined as a point of drastic changes in pair and radial deviations, diffusion constant, and of disappearance of the first Bragg peak, neither "melting" temperature $T_{\rm m}(N)$ nor scaled to 2D infinite system (8) melting temperature $T_{\rm m}^{\rm inf}(N)$ tends to first-order phase transition temperature in an infinite 2D system as the number of particles in the cluster increases;

(ii) function $T_{\rm m}(N)$ is not monotonic. The clusters with the maximal number of completed crystal shells and the minimal number of defects have maximal melting temperatures;

(iii) one can introduce the temperature $T_{\rm m}^{\rm inf}(r < r_{\rm c}(N)) \to T_{\rm m}^{\rm inf}, \quad N \to \infty$ which is the (scaled to 2D infinite system) melting temperature of a core, the free of defects central region $r < r_c(N)$ of a cluster.

These qualitative predictions are presented in Figure 10.

4.3 Cluster D_{37}

System D_{37} can be considered as an intermediate one between mesoscopic and macroscopic clusters. An analysis of the global minimum configuration (see Fig. 4) and of the structure of normal motions with the minimal eigenfrequency $\omega_{\rm min}$ leads to the seemingly unambiguous conclusion about the absence of the intershell orientational disordering. However, our calculation shows that the melting in this system is not a one-step process. Instead, the orientational melting takes place at the temperature $T = T^* \approx 0.01$ that is approximately three times lower than that of total melting $T_{\rm m} \approx 0.035 \pm 0.002$. The orientational disordering of *all* pairs of shells takes place at temperature T^*.

The reason for this "anomalous" behavior of cluster D_{37} can be elucidated by considering the structure of the lowest local minima configurations (*i.e.* the configurations with the lowest energy). We have noted above (see Fig. 4c) that global and local minima configurations differ in a *symmetry*, namely, any breaking of the ground state configuration down into shells leads to the necessity of viewing one or two particles (see Sect. 3) as interstitials interposed between shells of the cluster. Only two first shells are well-defined: $D_{37}(\underline{1,6},...)$. On the contrary, the configuration of the first excited state (of the lowest local minima with energy $\epsilon_{\rm loc}^{(1)} \approx 8.3325$) is rather symmetrical

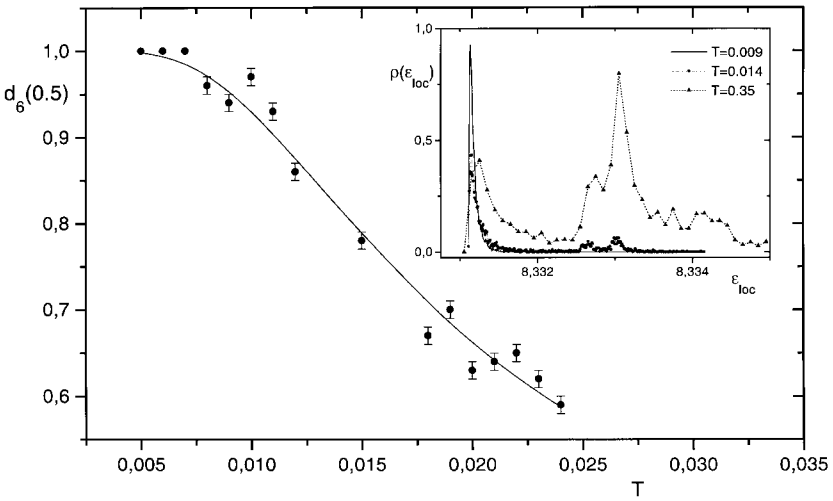

Fig. 11. The probability that the central particle of cluster D_{37} has six neighbours as a function of temperature T. In the inset local minima distributions for different temperatures are shown. One can see that at $T > 0.01$ a group of local minima with energies near $\epsilon^{(1)}$, the energy of the lowest local minimum, are being occupied.

and has the clear shell structure: $D_{37}^{(1)}(1, 7, 13, 16)$. As shells of the cluster in this local minimum are not faceted, it is not surprising that the motion (in this local minimum) with the lowest eigenfrequency $\omega_{\min}^{(1)} \approx 0.4$ corresponds to the intershell rotation. This is illustrated in Figure 4c.

Plotted in Figure 11 is the probability d_6 of the central particle having six neighbours. This figure shows that at temperatures $T > T^* = 0.01 \pm 0.002$ there is a finite probability to find a system in the vicinity of the local minimum $D_{37}^{(1)}(1, 7, ...)$. Yet another illustration of this rearrangement is the change in histogram $\rho(\epsilon_{\rm loc})$ of the local minima distribution [9] shown in the inset of Figure 11. One can see that at $T = T^*$ a spike at energy $\epsilon_{\rm loc}^{(1)}$ appears. Further increasing the temperature leads to the occupancy of other local minima and, at $T > 0.3$, the radial disordering takes place, particles interchange between shells and the radial distribution function is washed out. So, at $T > T^*$, a part of the time the system lives in the neighbourhood of the "symmetrical" local minimum that is *unstable* against intershell rotation at such high temperatures. This intershell disordering also manifests itself as a sharp increase in relative angular intershell deviations at this temperature $T = 0.01$.

From results of studies of atomic clusters [7–9] it is known that clusters of some specific number of particles (so-called "magic" Lennard-Jones (LJ) clusters such as LJ_{13}, LJ_{19}, see *e.g.* works [9] and references therein) have distinct regions of coexistence of "liquid-like" and "solid-like" forms when in a certain temperature interval there is nonzero probability to find the cluster either in a "liquid-like" or in a "solid-like" form. It was shown that this unusual property owes its origin to features of the multidimensional potential energy surface and stems from an existence of regions (well-separated by high barriers) in phase space with distinct physical properties and appreciable residence time for the system in each region.

A picture of disordering in cluster D_{37} with increasing temperature closely resembles the picture of structural transitions in magic number atomic clusters. Of course, at sufficiently high temperatures, at $T > T^* = 0.01$, the system can be found in one of two distinct regions in phase space with a barrier between them. This equilibrium can be described as:

$$D_{37}(\underline{1,6},\tilde{1},13,16) \overset{K}{\rightleftharpoons} D_{37}(1,7,13,16),$$
$$K = \frac{[D_{37}(1,7,13,16)]}{[D_{37}(\underline{1,6},\tilde{1},13,16)]} = \mathrm{e}^{-\Delta F(T)/T}$$

where $\Delta F(T)$ is free energy difference of "symmetrical" and "fully ordered" states of the cluster. At $T < 0.01$, constant of equilibrium $K \sim 1 - d_6$ is equal to zero and increases markedly as the temperature is increased (see Fig. 11).

Previous investigations of magic number atomic clusters have shown that two distinct phases can be said to coexist if a suitable order parameter Q can be found such that the probability distribution $p(Q)$ of the order parameter in the canonical ensemble has two maxima [9]. Figure 12 shows the variation of the Landau free energy $F(Q) = F(T) - T\ln(p(Q))$ as a function of the order parameter $Q = \Psi_6$ at a number of temperatures. In order to calculate the probability distribution $p(Q)$ we applied the method of the canonical distribution function sampling [9]. As the order parameter two-dimensional bond-orientation order parameter averaged over internal region $r < 2.4$ of the cluster has been used:

$$\Psi_6 = \left\langle \left| \frac{1}{N(r<2.5)} \sum_i \frac{1}{N_i} \sum_p^{N_i} \exp\left(\jmath 6\varphi_p\right) \right|^2 \right\rangle. \qquad (9)$$

The first sum in this equation is over $N(r < 2.5)$ particles from the region $r < 2.4$ (belonging to three inner shells), the sum on p is over N_i neighbours of the particle i,

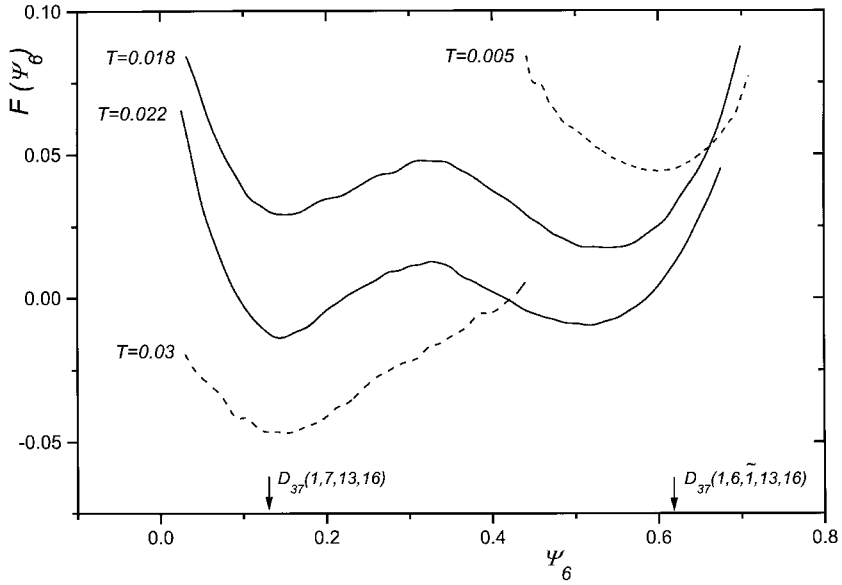

Fig. 12. Variation of the Landau free energy for D_{37} *vs.* 2D bond-orientation order parameter Ψ_6 at different temperatures T. As the Helmholtz free energy $F(T)$ is independent of Ψ_6, the zero of the Landau free energy at each temperature has been chosen so as to better represent the results.

and φ_p is the angle between the bond $\langle i,p\rangle$ and an arbitrary axis. The values of Ψ_6 lie between 0 and 1, where the latter case corresponds to a part of a perfect crystal.

Arrows in the figure indicate the values of the order parameter Ψ_6 corresponding to the ground state ($\Psi_6 \approx 0.63$) and to the lowest local minimum ($\Psi_6 \approx 0.13$). One can see that at $T = 0.018$ and $T = 0.022$ the Landau free energy has two minima, the "ordered" well (with higher value of Ψ_6) is preferable at $T = 0.018$. The dashed curves correspond to temperatures at which only one well was observed. We have found that the temperature region over which the cluster D_{37} shows double minima in the Landau free energy, and hence there are both stable and metastable states, can be estimated as $0.012 < T < 0.025$.

The above analysis suggests that, with the cluster D_{37} being radial ordered up to $T_{\rm m} = 0.035$, the temperature region $0.012 < T < 0.025$ *can not* be considered as the region of coexistence of its "solid-like" and "liquid-like" forms. Instead, this temperature interval can be thought of as the region of coexistence of "solid-like" and "orientationally disordered" forms. It is the presence of such a region that enables us to consider the system D_{37} as an intermediate one that has features of both mesoscopic and macroscopic clusters.

To conclude of this paragraph we note that the number of D_{37}-like "anomalous" systems can be varied by tuning the characteristic range of an interaction potential. Increasing the temperature in such systems can lead to structure rearrangements (with changes in symmetry), changes in the shell distribution or in types of defects. Consequently, the above consideration can be helpful in the study of thermodynamic properties of the clusters, parameters of interparticle potential of which can be varied in wide limits, *e.g.* of the system of electrons in a semiconductor dot near metal electrodes [5,6], dusty plasma clusters [31,32] etc.

5 Conclusion

We have presented the results of a numerical simulation of a finite 2D dipole system in parabolic confinement. Ground state configurations and the spectrum of normal modes of clusters of $N \leq 80$ particles have been found. An addition of particles to the system leads to a gradual filling of crystal shells of different symmetry. The clusters with minimal energies and maximal lowest eigenfrequencies are those with the maximal number of completely filled crystal shells and (in the case of large clusters, $N > 40$) with equal numbers of particles on the last two shells.

The character of disordering with increasing the temperature is markedly different for mesoscopic ($N < 37$) and macroscopic ($N > 37$) clusters. Particularly, mesoscopic clusters are characterized by an existence of two types of disordering effects: orientational and full (radial). Depending on the degree to which crystal shells are completed the temperatures of orientational "melting" of different pairs of shells can differ greatly from each other. Orientational melting in large systems is absent.

An analysis of the local minima distribution of the system D_{37} as a function of temperature has shown that this system has features of both mesoscopic and macroscopic clusters. Namely, there is a region of temperatures in which the cluster is in a dynamical equilibrium between "solid-like" and radial ordered but orientationally disordered forms.

The system of a large number of particles is nonuniform: both the characteristic interparticle distance and the local density of defects are functions of a distance

r from the center of the system. As a consequence, the temperature at which a sharp increase in radial and pair deviations starts, vanishing of the first Bragg peak takes place, and the diffusion of particles appear does not approach temperature $T_{\rm m}^{\rm inf}$ of a first-order phase transition in a 2D infinite dipole system as the number of particles is increased. The "melting" temperature $T_{\rm m}(N)$ is a nonmonotonic function of the number of particles N and is maximal for the clusters with the maximal number of completed crystal shells.

We wish to thank A.M. Popov and S.A. Verzakov for fruitful discussion. The work has been supported by Russian Foundation of Basic Research, INTAS and the Program "Physics of Solid Nanostructures".

References

1. P. Pieranski, Phys. Rev. Lett. **45**, 569 (1980).
2. L.A. Bol'shov *et al.*, Uspekhi Fiz. Nauk (*in Russian*) **122**, 125 (1977).
3. P.V. Anderson, in *Elementary Excitations in Solids, Molecules and Atoms A*, p. 1 (1974).
4. V.M. Agranovich, Yu.E. Lozovik, JETP Lett. **17**, 148 (1972); I.V. Lerner, Yu.E. Lozovik, Phys. Lett. A **64**, 483 (1978); Yu.E. Lozovik, V.I. Yudson, JETP Lett. **22**, 11 (1975).
5. R.C. Ashoori *et al.*, Phys. Rev. Lett. **68**, 3088 (1992); **71**, 613 (1993); N.B. Zhitenev *et al.*, preprint `cond-mat/9703241` (1997).
6. A.A. Koulakov, B.I. Shklovskii, Phys. Rev. B **57**, 2352 (1998).
7. T.L. Beck, J. Jellinek, R.S. Berry, J. Chem. Phys. **87**, 545 (1987).
8. D.J. Wales, R.S. Berry, Phys. Rev. Lett. **73**, 2875 (1994); M.A. Miller, D.J. Wales, J. Chem. Phys. **107**, 8568 (1997).
9. R.M. Lynden-Bell, D.J. Wales, J. Chem. Phys. **101**, 1460 (1994); J.P.K. Doe, D.J. Wales, J. Chem. Phys. **102**, 9673 (1995).
10. M. Sungik, G. Toulouse, A.A. Lucas, Sol. State Commun. **11**, 1629 (1972); J. Heinrichs, Phys. Rev. B **8**, 1346 (1973); J.C. Inkson, J. Vac. Sci. Technol. **11**, 943 (1974); D.L. Mills, Phys. Rev. B **15**, 763 (1977); I.V. Lerner, Yu.E. Lozovik, Fiz. Tv. Tela [Sov. Solid St. Phys.] **20**, 1293 (1978).
11. S. Kirkpatrick, C.D. Gelatt, M.P. Vecchi, Science **220**, 671 (1983); Y. Xiang, D.Y. Sun, W. Fan, X.G. Gong, Phys. Lett. A **233**, 216 (1997).
12. N.N. Kalitkin, *Numerical Methods* (*in Russian*) (Nauka, Moskow, 1978).
13. G. Bhanot, Rep. Prog. Phys. **51**, 429 (1988).
14. A. Goodman, D. Sokal, Phys. Rev. D **56**, 1024 (1987).
15. Yu.E. Lozovik, Uspekhi Fiz. Nauk (*in Russian*) **153**, 356 (1987); Yu.E. Lozovik, V.A. Mandelshtam, Phys. Lett. A **145**, 269 (1990); **165**, 469 (1992).
16. V.M. Bedanov, F.M. Peeters, Phys. Rev. B **49**, 2662 (1994); V. Shweigert, F.M. Peeters, Phys. Rev. B. **51**, 7700 (1995); I.V. Shweigert, V.A. Shweigert, F.M. Peeters, Phys. Rev. B **54**, 10827 (1996).
17. D.J. Wales, A.M. Lee, Phys. Rev. A **47**, 380 (1993).
18. D.H.E. Dubin, T.M. O'Neil, Rev. Mod. Phys. **71**, 87 (1999).
19. R. Calinon *et al.*, in *Ordering in Two Dimensions*, edited by S.K. Sinha (Elsevier, New York, 1980).
20. Y. Kondo *et al.*, Phys. Rev. Lett. **68**, 3331 (1992); G.E. Volovik, U. Parts, JETP Lett. **58**, 774 (1993).
21. Yu.E. Lozovik, E.A. Rakoch, Phys. Rev. B **57**, 1214 (1998).
22. Yu.E. Lozovik, E.A. Rakoch, Phys. Lett. A **235**, 55 (1997).
23. A.I. Belousov, Yu.E. Lozovik, JETP Lett. **68**, 817 (1998).
24. P.J. Steinhardt, D.R. Nelson, M. Ronchetti, Phys. Rev. B **28**, 784 (1983).
25. K.J. Standburg, Rev. Mod. Phys. **60**, 161 (1988).
26. C.J. Cerjan, W.H. Miller, J. Chem. Phys. **75**, 2800 (1981); W. Quapp, Chem. Phys. Lett. **253**, 286 (1996).
27. V.M. Bedanov, G.V. Gadiyak, Yu.E. Lozovik, Phys. Lett. A **92**, 400 (1982).
28. Yu.E. Lozovik, V.M. Farztdinov, Sol. State Commun. **54**, 725 (1985); Yu.E. Lozovik *et al.*, Phys. Lett. A **109**, 289 (1985).
29. To define an effective (mean) density of a cluster of not very large number of a particles ($N < 50$), when the nonuniformity of the local density is not essential, we consider the distance $|\delta\mathbf{k}|$ to the maximum of the structure factor, *i.e.* to the first Bragg peak for a "solid" cluster (when $T < T_{\rm m}$) or to the Lorentz peak in the case of a "liquid" cluster (when $T > T_{\rm m}$). The characteristic distance between particles in a cluster can be defined then as $a = 2\pi/|\delta\mathbf{k}| = \left[2/(n\sqrt{3})\right]^{1/2}$. The corresponding temperature of a 2D infinite system can be estimated as $T^{\rm inf} = k_{\rm b}T/(D^2n^{3/2}) \approx T\left[|\delta\mathbf{k}|/(2\pi)\right]^3/0.8$.
30. J.M. Caillol, Phys. Rev. Lett. **50**, 2086 (1983).
31. C.H. Chiang *et al.*, Phys. Rev. Lett. **77**, 646 (1996); W.-T. Juan *et al.*, Phys. Rev. E **58**, R6947 (1998).
32. L. Cardido, J.P. Rino, N. Studart, F.M. Peeters, J. Phys. Cond. Matt. **10**, 11627 (1998); G.E. Astracharchik, A.I. Belousov, Yu.E. Lozovik, Phys. Lett. A (in print, 1999).